

Periplakin-dependent re-organisation of keratin cytoskeleton and loss of collective migration in keratin-8-downregulated epithelial sheets

Heather A. Long^{*‡}, Veronika Boczonadi[‡], Lorna McInroy, Martin Goldberg and Arto Määttä[§]

Centre for Stem Cell Research and Regenerative Medicine, School of Biological and Biomedical Sciences, University of Durham, Durham, DH1 3LE, UK

^{*}Current address: Institute for Medical Sciences, University of Aberdeen, Aberdeen, AB25 2ZD, UK

[‡]These authors contributed equally to this paper

[§]Author for correspondence (e-mail: Arto.Maatta@durham.ac.uk)

Accepted 18 October 2006

Journal of Cell Science 119, 5147-5159 Published by The Company of Biologists 2006

doi:10.1242/jcs.03304

Summary

Collective migration of epithelial sheets requires maintenance of cell-cell junctions and co-ordination of the movement of the migrating front. We have investigated the role of keratin intermediate filaments and periplakin, a cytoskeletal linker protein, in the migration of simple epithelial cells. Scratch wounding induces bundling of keratins into a cable of tightly packed filaments adjacent to the free wound edge. Keratin re-organisation is preceded by a re-distribution of periplakin away from the free wound edge. Periplakin participates with dynamic changes in the keratin cytoskeleton via its C-terminal linker domain that co-localises with okadaic-acid-treated keratin granules. Stable expression of the periplakin C-terminal domain increases keratin bundling and Ser431 keratin

phosphorylation at wound edge resulting in a delay in wound closure. Ablation of periplakin by siRNA inhibits keratin cable formation and impairs wound closure. Knockdown of keratin 8 with siRNA results in (1) a loss of desmoplakin localisation at cell borders, (2) a failure of MCF-7 epithelial sheets to migrate as a collective unit and (3) accelerated wound closure in vimentin-positive HeLa and Panc-1 cell lines. Thus, keratin 8 is required for the maintenance of epithelial integrity during migration and periplakin participates in the re-organisation of keratins in migrating cells.

Key words: Intermediate filaments, Plakins, Epithelial migration, RNA-interference

Introduction

Epithelial sheet migration is a fundamentally important process in both morphogenesis and tissue repair. Collective cell migration closes scratch wounds in simple epithelial layers and is responsible for the epithelial dorsal hole closure in *Drosophila* and eyelid closure of mammalian embryos (Martin and Parkhurst, 2004; Friedl et al., 2004).

Cytoskeletal dynamics is a key cellular mechanism in cell migration. Epithelial cells maintain cadherin-mediated cell-cell junctions during collective migration and assemble an actin 'purse-string' cable at the wound edge (Martin and Lewis, 1992; Bement et al., 1993; Danjo and Gipson, 1998). Partly depending on the cell type and the size of the injury, wound closure is mediated either by actomyosin contraction of the purse-string, by lamellipodia protrusions from the wound edge cells or by a combination of both mechanisms (Fenteany et al., 2000). Despite advances in understanding the regulation of actin dynamics, there remain several important questions about collective migration, such as, how migration is coordinated while the intact epithelial nature of the wound edge is retained.

Intermediate filaments (IFs), named after their 10-12 nm diameter size, constitute the main cytoskeletal network responsible for mechanical integrity of various tissues (Owens and Lane, 2003; Chang and Goldman, 2004; Toivola et al., 2005). Furthermore, IFs are required for polarised positioning of apical epithelial proteins in gut epithelia (Salas et al., 1997;

Toivola et al., 2004). Thus, one would expect that IFs participate in the maintenance of the integrity and polarity of the collectively migrating epithelial sheets.

Several studies indicate a role for keratin IFs in moderating cell migration. Epidermolysis bullosa simplex cell lines carrying mutations in either K14 or K5 keratin migrate faster in a scratch wound assay than a control keratinocyte cell line (Morley et al., 2003). Ablation of K6 by gene targeting of both K6a and K6b isoforms reveals that K6 negative cells display enhanced motility in vitro (Wong and Coulombe, 2003). Simple epithelial keratins have also been implicated in cell migration. Expression of K8 and K18 in mouse L fibroblasts and in melanoma cells increases the invasiveness of the transfected cells (Chu et al., 1993; Chu et al., 1996) and perinuclear re-organisation of K8/18 network by sphingosylphosphorylcholine increases cellular elasticity and augments migration through limited-sized pores (Beil et al., 2003). However, the studies on simple epithelial keratins have not fully addressed the role of IF networks in collective migration of simple epithelial sheets.

IF networks are connected to cell-cell and cell-matrix junctions by cytoskeletal linker proteins. The plakin family of cytolinkers comprises seven genes, plectin, desmoplakin, BPAG-1, envoplakin, periplakin and epiplakin, some of which encode for several protein isoforms (Leung et al., 2002). Plakins are large, rod-like proteins that are targeted to cellular

junctions by their N-terminal plakin domain. Most plakins, apart from spectraplakins, have a central coiled coil rod and a C-terminal IF-binding domain (Leung et al., 2002). Studies addressing plakins in cell motility have indicated profound effects on migration. BPAG-1 knockout mice have a wound-healing defect (Guo et al., 1995). Plectin^{-/-} fibroblasts display defects in their ability to reorganise actin microfilaments after activation of rac/rho/cdc42 signalling cascades which results in a reduced motility of plectin deficient cells (Andra et al., 1998). More recently, generation of isoform-specific knockouts for plectin have demonstrated that plectin-1 is involved in migration of both fibroblasts and T-lymphocytes and is required for efficient leucocyte infiltration to wounds (Abrahamsberg et al., 2005).

Periplakin was originally identified as a cornified envelope precursor and is targeted in cultured keratinocytes to cell membranes that surround core desmosomes (Ruhrberg et al., 1997). The periplakin C-terminus is the shortest among the family members comprising only the linker domain (Ruhrberg et al., 1997). However, this minimal IF-binding domain is able to interact with intermediate filaments both *in vivo* and *in vitro* (DiColandrea et al., 2000; Kazerounian et al., 2002; Karashima and Watt, 2002). Unexpectedly, periplakin associates with cortical actin network in keratinocytes even though the protein lacks a classical actin-binding domain (DiColandrea et al., 2000). Thus, periplakin is another candidate protein to mediate linkages between cytoskeletal networks in migrating cells.

In this study, we examined the role of keratin IFs and plakin proteins in the migration of scratch wounded epithelial cell sheets. To define the role of periplakin in the modulation of IF organisation, we downregulated the expression of periplakin by RNA interference. Furthermore, we generated stable cell lines expressing the periplakin C-terminal, IF-binding domain to elucidate its role in cytoskeletal organisation during epithelial sheet migration. Finally, to answer the question about the role of an intact IF network in simple epithelia, we downregulated keratin K8 expression by RNA interference in MCF-7, HeLa and Panc-1 cells.

Results

Re-organisation of keratin cytoskeleton during epithelial migration

Initial scratch wounding experiments using MCF-7 mammary adenocarcinoma cell line revealed that most changes associated with re-organisation of the IF cytoskeleton can be studied at the 30 minutes and 2 hour time points after wounding. These time points were routinely used thereafter. We established that MCF-7 monolayer wounds behave like previously described wounds of simple epithelial monolayers (Bement et al., 1993; Danjo and Gibson, 1998; Fentenay et al., 2000) by assembling an actin cable at the wound edge that was present at both 30 minutes (Fig. 1A) and 2 hours (Fig. 1B). Most wound edge cells had only limited number of small lamellipodia-like protrusions but exhibited a large number of microspikes when studied by scanning electron microscopy (Fig. 1C). In the same set of experiments, we investigated the organisation of the IF cytoskeleton. We initially noticed that at the 2 hours time-point keratin 8/18 filaments were re-arranged to a thick cable-like bundle at the wound edge (Fig. 1D). The subsequent analysis revealed that at 30 minutes time point most wound edge cells had more intense staining for keratin than cells in the

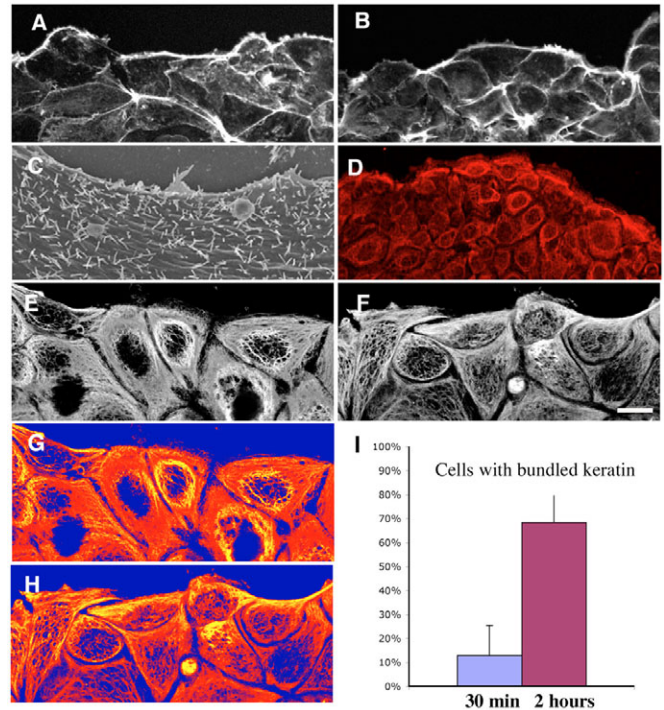


Fig. 1. Cytoskeletal organisation at MCF-7 scratch wound edges. (A) Phalloidin-stained actin cytoskeleton 30 minutes after wounding. (B) Actin cytoskeleton 2 hours after wounding. (C) SEM image of the cell surface of a wound edge cell 30 minutes after wounding displaying numerous microspikes but only a few small lamellipodia. (D-H) Immunofluorescence staining of Keratin 8 at the wound edge. (D) Low-power overview of K8 network at wounded epithelia 2 hours after wounding. (E) High-power image of K8 at the wound edge 30 minutes after wounding. (F) K8 at the wound edge 2 hours after wounding. (G) Pseudocolour gradient representation of the staining intensity from panel E. Yellow colour marks the most intense staining that is mostly localised at a cage around the nucleus. (H) Pseudocolour gradient representation of the staining intensity from panel F showing most intense keratin staining at the wound edge. (I) Percentage of cells showing the strongly stained keratin cable immediately parallel to the wound edge 30 minutes and 2 hours after the wounding. 200 cells were scored from three independent wounds. The scale bar shown in F equals to 20 μ m in A, B, E-H; 50 μ m in D and 200 nm in C.

monolayer further away from the wound. While some wound edge cells had already re-arranged the keratin IF network to include a few filaments parallel to the wound edge, the strongest staining for keratin at the 30 minutes time point was observed in a cage-like network around the nucleus (Fig. 1E). At 2 hours after wounding, the majority of the wound edge cells had a thick cable of bundled keratin filaments that ran parallel to the wound edge (Fig. 1F). This observation was confirmed by counting cells with keratin bundles at wound edge and analysing fluorescence intensity in micrographs where the gradient of intensity was converted to pseudocolour images. Panels 1G and 1H represent the intensity gradients of panels 1E and 1F, respectively, revealing how the highest intensity of keratin immunofluorescence shifts to the wound edge bundles. On average, over 70% of wound edge cells displayed a prominent keratin bundle at the 2 hours time point (Fig. 1I).

Field emission scanning electron microscopy was employed to investigate the detailed organisation of keratins at the wound edge. To this end, cell membranes were extracted and the actin cytoskeleton was digested by incubation with gelsolin (Svitkina et al., 1996). The ultrastructure of non-extracted cells did not change noticeably at the early stages of wound healing after the initial induction of microspikes, filopodia and membrane ruffling (Fig. 1C). By contrast, the detergent-extracted and actin-depleted cells revealed that a marked re-organisation of the keratin network takes place between 30 minutes and 2 hours. At 30 minutes, the IFs formed a loosely organised network throughout the cell (Fig. 2A). Many cells had one or a few filaments aligned at the wound edge but no further bundling of the filaments was observed in these cells (Fig. 2B). After 2 hours the majority of the cells displayed a zone of bundled IFs parallel to the wound edge (Fig. 2C-E). We observed bundled zones with aligned filaments up to 1 μm wide. Finally, high magnification (200,000 \times) was utilised to confirm that the visualised filaments were between 10 and 20 nm wide (Fig. 2F). Thus, the presence of the keratin cable observed at the wound edge by immunofluorescence staining (Fig. 1) was confirmed by field emission scanning electron microscopy.

Differential re-distribution of desmoplakin and periplakin at the wound edge

Intermediate filaments connect to desmosomes, the major epithelial cell-cell junction, via plakin cytoskeletal linker proteins. The main desmosomal plaque protein, desmoplakin is required for integrity of epithelial and endothelial tissues (Gallicano et al., 1998; Vasioukhin et al., 2001; Zhou et al., 2004). Another plakin, periplakin, is localised around the core desmosome in epidermal cells and is upregulated in cells that need to withstand mechanical forces such as the differentiated suprabasal keratinocytes and the umbrella cells that form the lining of the bladder (Ruhrberg et al., 1997; Aho et al., 1998; DiColandrea et al., 2000). We reasoned that the re-organisation of IF network could be associated with or influenced by a change in the subcellular distribution of cytoskeletal linker proteins and investigated the subcellular distribution of plakin proteins in intact monolayers and wound edges.

In unwounded epithelial monolayers, periplakin and desmoplakin were partially co-localised at cell borders (Fig. 3A). Likewise, a partial co-localisation of periplakin and β -catenin, an adherens junction protein, could be seen in double immunofluorescence staining (Fig. 3C). Visualisation of XZ-projections of the cell borders by confocal microscopy confirmed that there is a partial overlap of periplakin distribution with both desmoplakin and β -catenin. (Fig. 3A,C). Specifically, desmoplakin expression extended higher in the apical aspect of the lateral cell border than periplakin. This is in agreement with the previously reported periplakin distribution at keratinocyte cell membranes, where periplakin staining surrounds desmosomes and only partially co-localises with desmoplakin (Ruhrberg et al., 1997). In addition to cell border staining, a substantial proportion of periplakin was localised in a cytoplasmic pool (Fig. 3B). In monolayers, the cytoplasmic periplakin did not co-localise with either keratin intermediate filament network (Fig. 3B) or actin cytoskeleton (Fig. 3D).

Periplakin and desmoplakin show different dynamics in their

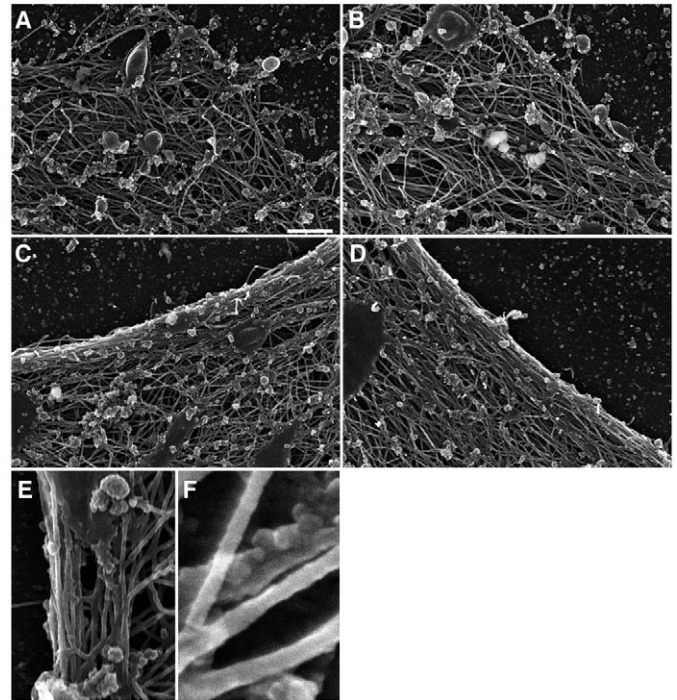
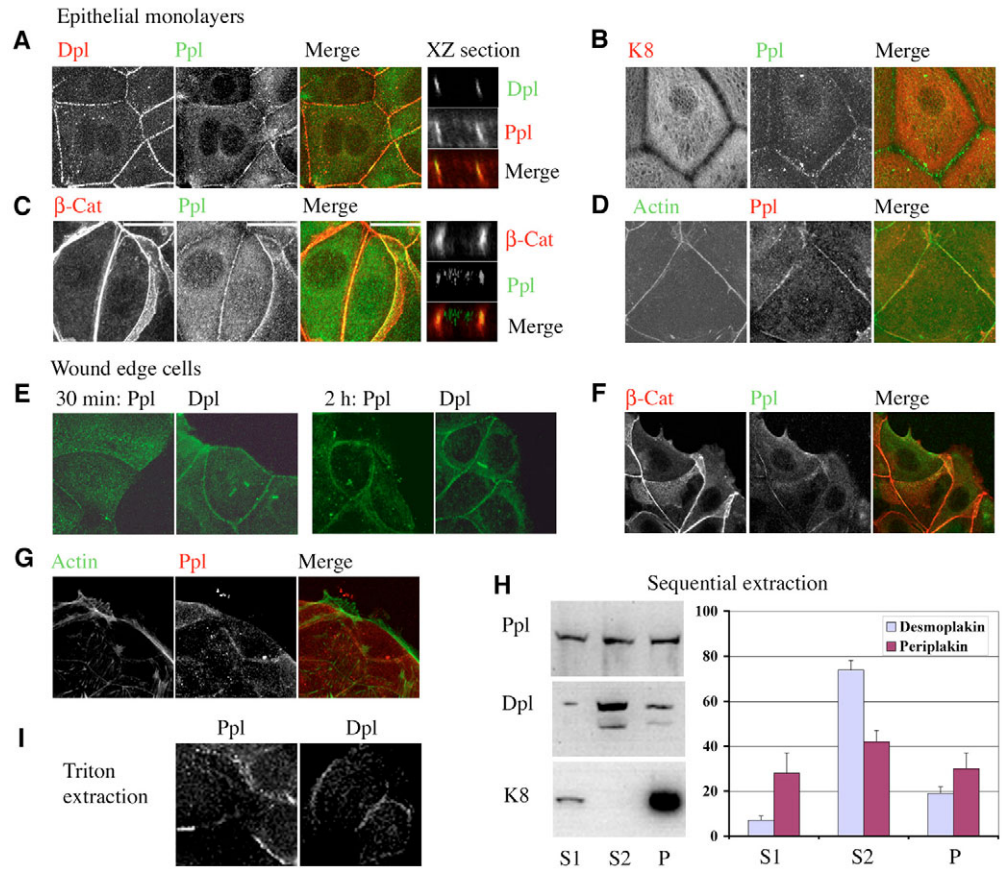


Fig. 2. Field emission scanning electron microscopy of the intermediate filament network at MCF-7 scratch wound edges. Confluent monolayers grown on silicone discs were scratch wounded. After 30 minutes or 2 hours the cells were extracted and depleted from filamentous actin. (A,B) Two representative examples of the wound edge IF cytoskeleton 30 minutes after wounding. (C,D) Two examples of IF organization at the wound edge 2 hours after the wounding. (E) High magnification of the keratin cable at the wound edge. (F) Individual chromium-coated filaments at 200,000 \times magnification. The scale bar corresponds to 500 nm in A-D, 175 nm in E and 55 nm in F.

re-distribution after wounding. Desmoplakin was still prominently retained at the free wound edge 30 minutes after wounding (Fig. 3E), whereas periplakin staining was uniformly cytoplasmic in the wound edge cells (Fig. 3E). Notably, the cell-cell junctions were still retained two hours after wounding as only the free wound edge was free of periplakin and desmoplakin staining (Fig. 3E). The dynamics of periplakin resembled the behaviour of adherens junction proteins, such as β -catenin that was not localised at the free wound edge 30 minutes after the wounding (Fig. 3F). Thus, periplakin re-distribution precedes the re-arrangement of intermediate filaments. The cytoplasmic pool of periplakin did not co-localise with actin cytoskeleton at the wound edge (Fig. 3G), indicating a different role for periplakin in simple epithelial cells compared with keratinocytes, where periplakin is co-localised with cortical actin (DiColandrea et al., 2000).

Cellular fractionation studies supported the finding that periplakin and desmoplakin show differential distribution in MCF-7 cells. Periplakin was distributed in approximately equal proportions in the saponin-soluble cytosolic pool, the Triton-X100 soluble pool and in the Triton-X insoluble cytoskeletal pool (Fig. 3H), whereas more desmoplakin was present in the Triton-soluble than saponin-soluble pool (Fig. 3H). Although slightly more periplakin than desmoplakin was

Fig. 3. Periplakin expression in MCF-7 monolayers and wound edges. (A-D) Intact monolayers were stained with (A) Desmoplakin and periplakin (red and green channels and merged image); XZ-projection confirms partial co-localisation the two plakins at cell borders. Note also the distinct cytoplasmic pool of periplakin. (B) Keratin 8 and Periplakin. (C) Periplakin and β -catenin, (D) Actin and periplakin. Note that cytoplasmic periplakin is not co-localised with either keratin or actin networks in monolayer cells. (E-G) Wound edge cells stained with (E) Periplakin (left panel at both time points) and desmoplakin (right at both time points) 30 minutes and 2 hours after wounding. Desmoplakin, unlike periplakin is retained at the free wound edge at the 30 minutes time point. (F) Periplakin (green) and β -catenin (red) merged image, 30 minutes after wounding. (G) Periplakin (red) and Actin (green), 2 hours after wounding. (H) western blot of the subcellular distribution of periplakin (Ppl), Desmoplakin (Dpl) and Keratin 18 (K18) in Saponin-soluble (S1 pool), Triton X-100 soluble (S2 pool) and insoluble pools (P3). Quantification of the relative distribution of periplakin and desmoplakin in the fractions was performed by densitometry of four independent fractionation experiments. (I) Immunofluorescence staining of cell extracted on coverslips confirming that Triton-insoluble periplakin (left panel) and desmoplakin (right panel) are located at cell borders.



detected in the Triton-insoluble pool, both proteins were present at cell borders after detergent extraction (Fig. 3I).

Periplakin-C-termini bundle keratin intermediate filaments and localise in okadaic-acid-treated keratin granules

We next investigated the role of periplakin in keratin dynamics in cells at the wound edge. Since the N-terminus of periplakin mediates association with desmosomes and other membrane locations and the C-terminus of periplakin alone shows a constitutive binding to IFs, we focused on whether there are any effects on keratin re-organisation by the C-terminal linker domain. In addition to Ppl-HA constructs described earlier (DiColandrea et al., 2000) we generated EGFP-Ppl-C-terminal construct to follow the dynamics of the periplakin linker domain (Fig. 4A).

In transient transfections, the EGFP-tagged periplakin linker domain was associated with keratin cytoskeleton (Fig. 4B), indicating that the interaction of periplakin C-terminus and keratin filaments can take place in MCF-7 cells. Surprisingly, transiently transfected monolayers that were subsequently wounded contained only a few GFP positive cells at wound edges. In the initial experiments, where the transfection efficiency varied between 22 and 46%, only 5% (7 out of 144) of wound edge cells expressed high levels of the construct. Moreover, when present in high levels at wound edge cells,

EGFP-PPL-C protein could be detected in aggregates together with collapsed keratin filaments (Fig. 4B). Thus, over-expression of periplakin by transient transfection appeared to interfere with the keratin organisation in the wound edge cells and prompted us to study the role of periplakin C-terminus in detail.

The observed aggregates of periplakin and keratins were reminiscent of keratin granules that are formed by manipulating phosphorylation status of IFs (Yatsunami et al., 1993; Liao et al., 1997; Strnad et al., 2001; Strnad et al., 2002). Consequently, we investigated periplakin localisation in okadaic acid (OA)-treated cells. The endogenous periplakin was found co-localised with OA-induced keratin granules at the wound edge cells (Fig. 4C). Notably, many cells maintained membrane-associated periplakin while aggregating the cytoplasmic and/or cytoskeletal periplakin pool with keratins (Fig. 4C). Further evidence for a re-distribution of periplakin in okadaic-acid-treated cells was obtained by fractionating OA treated MCF-7 monolayers where periplakin could no longer be detected in the Triton-insoluble cytoskeletal pool (Fig. 4D). Thus, protein phosphorylation appears to regulate the subcellular distribution and interactions of periplakin with keratin cytoskeleton.

The association of periplakin in the OA-induced cytoskeletal granules was dependent on the periplakin C-terminus. In transient transfections both HA-tagged (Fig. 4E) and EGFP-

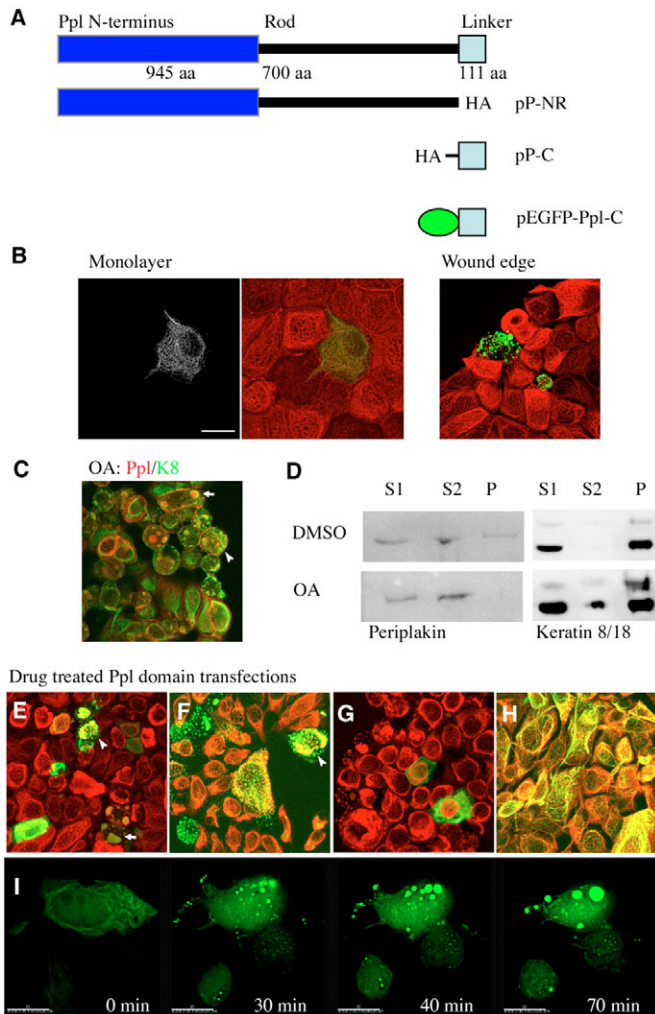


Fig. 4. Co-aggregation of keratin and periplakin in Okadaic acid-treated MCF-7 cells. (A) Periplakin (Ppl) domain constructs used in transfection experiments. HA, haemagglutinin tag; Linker; the C-terminal tail of periplakin comprising the IF-binding domain (Ruhberg et al., 1997; DiColandrea et al., 2000); Green oval, Enhanced Green Fluorescence Protein. (B) EGFP-Ppl C construct (green) and Keratin 8 (red) in MCF-7 cells. Monolayer panel: left side; EGFP fluorescence, right side; merged image. Wound edge panel: merged image of EGFP-PplC and K8 (red), note the aggregated keratin cytoskeleton in the wound edge cell. (C) Okadaic acid-treated wound edge stained for endogenous periplakin (red) and keratin 8 (green) expression. Periplakin expression is retained at cell borders, whereas the cytoplasmic pool is concentrated in small aggregates (arrowhead) or larger inclusions (arrow). (D) Subcellular fractionation of Okadaic acid and vehicle (DMSO) treated MCF-7 monolayers. S1, Saponin soluble fraction; S2, Triton X-100 soluble fraction; P, Triton insoluble pellet. (E) Transient transfection of EGFP-PplC treated with Okadaic acid. Merged image of EGFP (green) and Keratin immunofluorescence (red). Note similar aggregates (arrowhead) and large inclusion (arrow) to those seen in panel C. (F) Transient transfection of pP-C treated with Okadaic acid. Merged image of HA-tagged Ppl linker domain (green) and Keratin immunofluorescence (red). (G) Transient transfection of pP-NR treated with Okadaic acid. Merged image of HA-tagged Periplakin without linker domain (green) and Keratin immunofluorescence (red). (H) Transient transfection of pP-C treated with SB. Merged image of HA-tagged periplakin linker domain (green) and Keratin immunofluorescence (red). (I) Still images taken at indicated time points from live cell imaging of pEGFP-PplC transfection treated with Okadaic acid.

tagged (Fig. 4F) periplakin linker domains associated with keratin granules upon OA treatment whereas the PPL-NR construct lacking the C-terminal linker domain did not co-localise with keratins (Fig. 4G). Moreover, a drug that regulates phosphorylation status of keratins without collapsing the IF network, p38 MAPK inhibitor SB203580, did not interfere with interaction of periplakin linker and keratins (Fig. 4H). Finally, live cell imaging was used to confirm the formation of the aggregates after OA application (Fig. 4I). Initially EGFP-tagged periplakin C-terminus localised with intermediate filaments (Fig. 4I, 0 minutes). Subsequently EGFP-containing granules started appearing and grew larger (Fig. 4I, 30 minutes, 40 minutes and 70 minutes). Thus, the periplakin C-terminus is not non-specifically trapped in keratin granules but is associated with the filaments prior to drug treatment and co-aggregates with keratins.

Stable expression of the periplakin linker domain interferes with keratin reorganisation at wound edge

To investigate further the effect of periplakin linker domain on the keratin re-organisation at the wound edge we generated stable MCF-7 clones expressing HA-tagged periplakin C-terminus (Fig. 5A). We investigated the closure of scratch wounds in two independent cell lines expressing pHA-Ppl-C plasmid. Compared with a control clone transfected with

empty pCiNeo vector (Fig. 5B,C), the clones expressing periplakin C-terminus showed a consistent delay in wound closure (Fig. 5B,C). The slower migration of the epithelial sheets was associated with abnormal organisation of keratin filaments at the wound edge. At 30 minutes after wounding, the epithelia transfected with empty vector had a well-organised keratin cytoskeleton and had started to re-arrange the keratin cable parallel to the wound edge (Fig. 5Da). By contrast, the wound edge cells expressing periplakin C-terminus showed a variable phenotype comprising cells with either very thick irregular keratin bundles or keratin aggregates reminiscent of OA-induced keratin granules (Fig. 5Db,c). The increased bundling of keratin filaments was associated with a change in the distribution and amount of Ser431 phosphorylated keratins. Wound edge staining with a Ser431-specific phosphokeratin antibody demonstrated that keratin bundles in control transfected MCF-7 cells contained phosphorylated keratin (Fig. 5Ea). Stable cell lines expressing the periplakin C-terminus had thick phosphokeratin bundles throughout the wound edge cells and, furthermore, displayed bundled or collapsed phosphokeratin filaments in cells further away from the scratch wound (Fig. 5Eb). The increase in keratin phosphorylation in periplakin-transfected cells was also evident by western blotting experiments that confirmed that wounded C-terminal stable cells had induced Ser431 phosphorylation (Fig. 5F).

Downregulation of periplakin and keratin 8 expression by siRNA transfections

To assess the respective roles of IFs and associated plakins in the maintenance of epithelial integrity and during collective migration, we downregulated the expression of K8 and

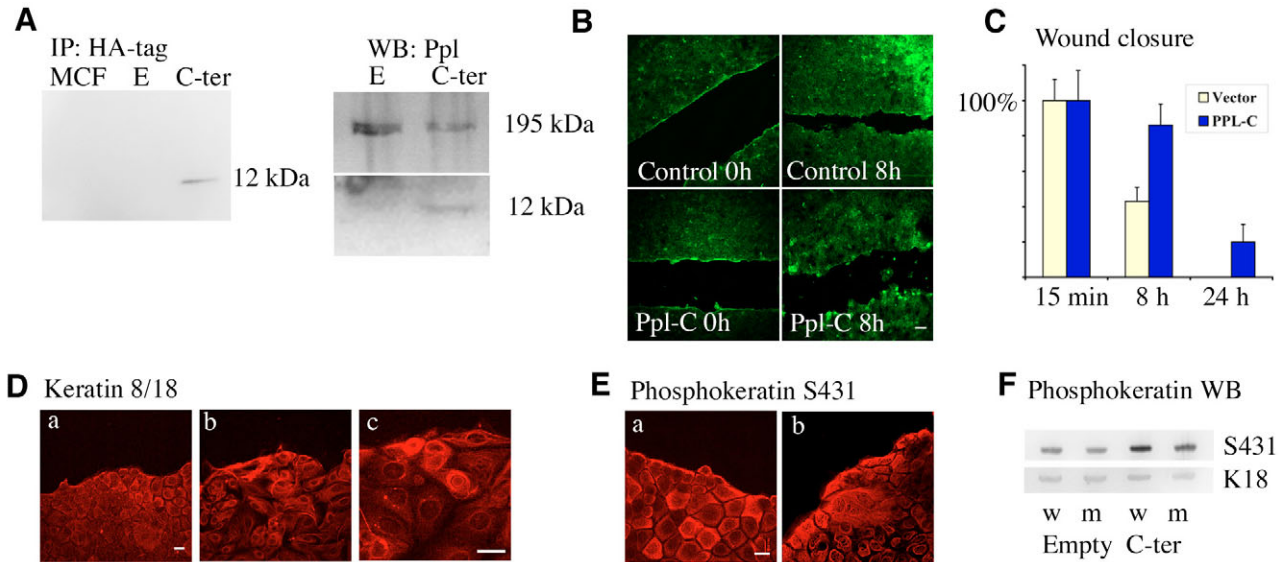


Fig. 5. Wound closure and keratin organisation in stable cell lines expressing PPL C-terminus. (A) Immunoprecipitation and western blot of Periplakin C-terminal linker domain by HA-tag antibody. MCF, untransfected parental cells; E, empty vector transfected clone, C-ter, representative clone of the linker domain transfected cells. Right panel: western blotting of endogenous periplakin and C-terminal domain with TD2 antibody. (B) Wound closure in control and Ppl-C cell lines. Wounded monolayers grown on glass coverslips were stained with FITC-phalloidin to visualise the wound edges. (C) Quantification of the wound closure in empty vector and PPL C-terminus transfected cell clones. Confluent monolayers grown in 6-well plates were wounded with pipette tip. The wound closure was followed by photographing phase contrast microscope fields after 15 minutes, 8 and 24 hours. For each wound the width of the wound after 15 minutes was designated as 100% and the subsequent time-points in the graph show the relative width of the open wound. Mean and standard deviation of ten measurements are shown. By the 24 hours time-point the control wounds were completely closed. (D) Keratin 8 immunofluorescence at wound edges. Panel (a) empty vector transfected control cell line. Panels (b) and (c) Keratin immunofluorescence at the edges of two independent wounds of a clone expressing periplakin C-terminus. (E) Ser431-phosphorylated keratin expression at wound edges. Panel (a) control; panel (b) cell line expressing Ppl C-terminus. (F) western blotting of Ser-431 phosphorylated keratin in monolayers (m) and wounded (w, ten wounds per 100 mm cell culture dish) control and Ppl C-terminal cell clones. Keratin 18 blot of the same membrane shows that there is no difference in the total keratin expression between the cell clones or treatments. Scale bar is 100 μ m in B, C, E and F and 20 μ m in G-K.

periplakin by siRNA transfections. We used three different target sites in the periplakin mRNA and compared specific siRNA oligonucleotides with a scrambled non-specific oligonucleotide. All periplakin siRNA oligonucleotides were effective and resulted in almost complete loss of periplakin protein expression (Fig. 6A and data not shown). The downregulation of periplakin appeared specific because desmoplakin expression levels remained unchanged (Fig. 6A). Only one of the tested K8 siRNAs resulted in a reduction of the expression to about 20–50% (depending on the confluency of the cells at the time of transfection; data not shown) of the control level in the total pool of transfected and non-transfected MCF-7 cells (Fig. 6A).

Immunofluorescence analysis of the transfected cells that had reached confluence forming an epithelial monolayer indicated that control transfections (Fig. 6B, top row) or ablation of periplakin (Fig. 6, middle row) did not have any discernible effect on epithelial morphology or the organisation of keratin IF network. On the contrary, transient transfections of siRNA duplexes targeted against K8 revealed that the keratin IF network is required for the maintenance of the epithelial sheet architecture of MCF-7 cells. Immunofluorescence analysis of the transfected cells showed a variable degree of loss of IFs in the cells with the majority of the cells having clearly reduced level of keratin staining (Fig. 6B). Notably, the residual IFs in the K8 siRNA transfected cells were

unorganised and appeared collapsed or bundled. The siRNA downregulation was specific for K8; western blot analysis of selected cytoskeletal proteins indicated that the expression of desmoplakin (not shown) and periplakin (Fig. 6A) remained unchanged in K8 siRNA transfected cells. Another K8 oligonucleotide that we tested did not downregulate K8 expression levels in the studied time-points. Transfections of this sub-optimal oligonucleotide did not result in any changes in intermediate filament architecture and were undistinguishable from control siRNA transfections (data not shown). Thus, a disruption of IF network was only seen when K8 levels were downregulated by an effective oligonucleotide.

An immediate observation of the siRNA transfected plates was that downregulation of K8 results in a disrupted epithelial sheet with reduced cell-cell contacts and appearance of cells with a non-epithelial, irregularly spread morphology (Fig. 6B). We reasoned that this could be due to either a failure of the cells to establish and maintain cell-cell junctions in the absence of proper IF network or altered cell survival and proliferation of keratin ablated cells. To study these possibilities further we first analysed the distribution of cell-cell junction proteins in K8 siRNA cells. Even though Western Blot analysis had indicated that the expression levels of desmoplakin and periplakin were unaffected by K8 downregulation, a clear change in the subcellular distribution of these proteins was observed. Both periplakin (Fig. 6B, bottom row) and

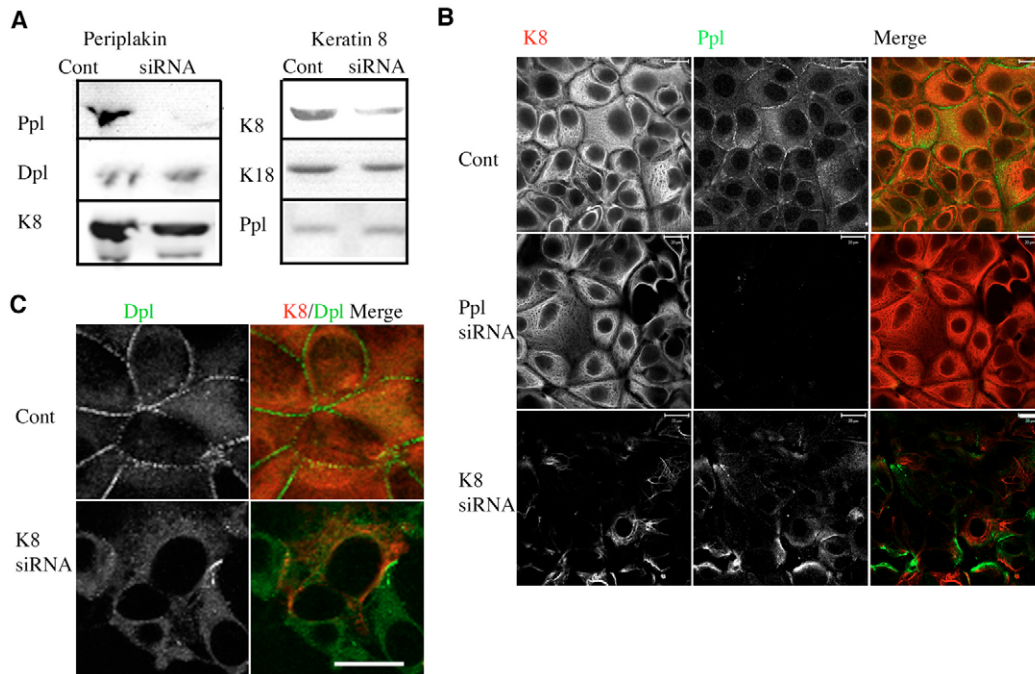


Fig. 6. Downregulation of periplakin and keratin 8 expression by siRNA transfections. (A) western blotting of total cell extracts from transient transfections with control or specific siRNAs. Total cell extracts were collected 72 hours after transfection and 20 μg protein aliquots were blotted with antibodies against indicated proteins. (B) Immunofluorescence staining of MCF-7 cells transfected with scrambled control siRNA (top row), Periplakin siRNA (middle row) or K8 siRNA (bottom row) showing K8 staining (red channel on the left) Periplakin staining (green channel, middle column) and merged image (on the right). (C) Control and K8 siRNA transfected cells stained with Desmoplakin antibody (green channel, on the left) and merged with K8 antibody staining (red channel). Scale bar is 20 μm in both B and C.

desmoplakin (Fig. 6C) were mostly cytoplasmic in K8 siRNA cells indicating that the disruption of the intermediate filaments had resulted in disruption of desmosomes and re-distribution of desmosomal plakins. Thus, downregulation of K8 expression leads to a loss of epithelial integrity.

Ablation of periplakin inhibits keratin re-organisation at wound edge cells and impairs wound closure

Although almost complete ablation of periplakin did not affect epithelial integrity it resulted in a cytoskeletal phenotype in the wound edge cells. Control siRNA transfected monolayers that were wounded 72 hours after transfection were able to re-arrange their keratin filaments at the wound edge into bundles parallel to the wound (Fig. 7A). Periplakin siRNA transfected cells did not re-arrange keratin filaments showing no keratin bundling or upregulation of the expression at the wound edge (Fig. 7B). The failure to re-arrange IF cytoskeleton was also evident in quantitative analysis where fluorescence intensity of keratin staining in monolayer five rows of cells away from the wound edge was compared with staining intensity at the area with filament bundles at the wound edge (Fig. 7C). In wounded monolayers transfected with control siRNA, the keratin bundling was evident by on average 3.5 times more intense fluorescence at the wound edge bundles. In the periplakin downregulated cells, however, there was no difference in keratin staining intensity between wound edge and cells away from the wound site (Fig. 7C). Thus, periplakin appears to be required for the re-organisation of keratin IF network at the wound edge of simple epithelial cell monolayers.

To ensure that any effect on epithelial morphology or wound closure was not due to decreased cell survival after periplakin or K8 downregulation, we analysed cell survival 48 hours after the transfections. Both periplakin and K8 siRNA transfected cells had similar, only slightly lower survival compared with control transfected or untransfected cells (Fig. 7D). Since periplakin siRNA transfected cells did not have any effect on the integrity of the monolayer we concluded that the effects seen in keratin 8 downregulated cells were not due to decreased cell survival.

To investigate the effect of periplakin knockdown on wound closure, we scratch wounded epithelial sheets transfected with periplakin or control siRNAs. Loss of periplakin impaired wound closure. Even 20 hours after the wounding, periplakin siRNA transfected scratch wounds remained mostly open (Fig. 7E,F). This result was also seen in wounded HeLa monolayers (Fig. 7F), indicating that periplakin regulates simple epithelial wound closure in general and not only in MCF-7 cells. The periplakin ablated wounds displayed uneven migration characterised by irregular wound edges that, nevertheless, retained cell-cell contacts between the wound edge cells (Fig. 7E). Thus, it is possible that periplakin-dependent keratin bundling participates in the maintenance of co-ordinated migration of the wound edge cells.

Collective migration is impaired in keratin-8-siRNA-transfected MCF-7 cells

The experiments where siRNA downregulation of K8 had disrupted the maintenance of MCF-7 epithelial sheets

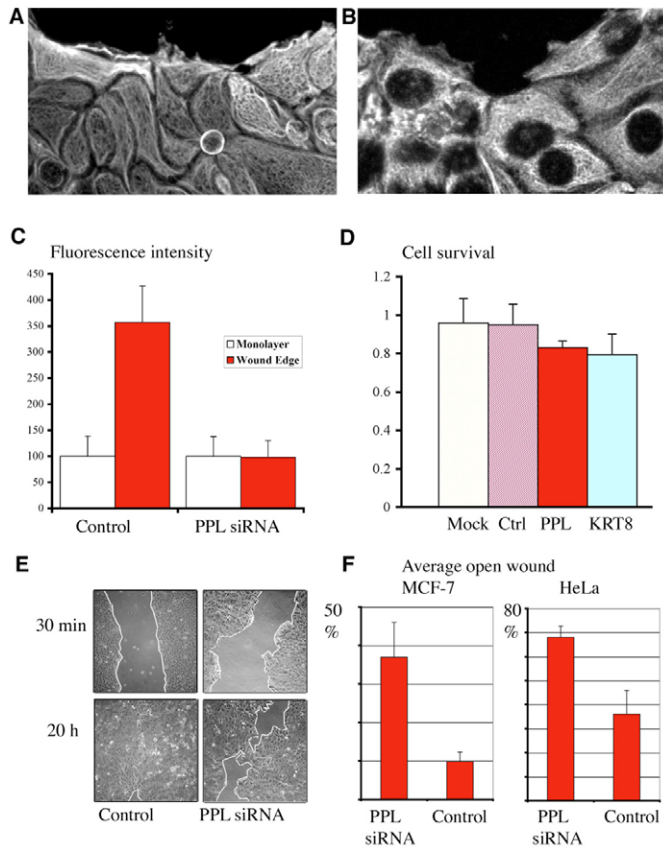


Fig. 7. Keratin organisation in periplakin siRNA transfected wound edge cells. Transiently transfected cells that had reached confluency were wounded 72 hours after transfection. (A) K8 immunofluorescence in control transfected cells. (B) K8 immunofluorescence in periplakin siRNA transfected cells. (C) Fluorescence intensity at wound edge compared with monolayer (adjusted to 100%) in control and periplakin siRNA transfected cells. Fluorescence intensity was measured in Image J programme from raw Zeiss LSM 510 images (Merged Z-stacks) from 20 cells in three independent wounds at wound edge and in epithelial monolayer 5 to 7 cell rows away from the wound edge. (D) Cell survival after siRNA transfections. Cell survival was measured using CellTiter cell proliferation kit (Promega). Mean and standard deviation (absorbance units at 490 nm) of three measurements are shown. (E) Phase contrast microscopic images of scratch wound closure of control and Periplakin siRNA transfected MCF-7 monolayers. (F) Quantification of the wound closure in MCF-7 and HeLa cells. The width of the wounds at 20 hours time point were measured from photomicrographs and displayed as percentage of remaining wound width from the start of the assay. Mean and s.e.m. from three independent transfections are shown.

suggested that the collective nature of the migration of MCF-7 epithelia could also be affected. At early time points of the wound closure, the control siRNA and K8 siRNA transfected epithelia migrated as a uniform row of cells (Fig. 8A) but in the subsequent time points the loss of epithelial integrity in the keratin 8 siRNA transfected cells became evident. Interestingly, the loss of cell-cell contacts in the migrating sheet resulted in individual cells breaking away from the epithelial front and apparently migrating faster in the wound area (Fig. 8A). However, the keratin-negative cells failed to

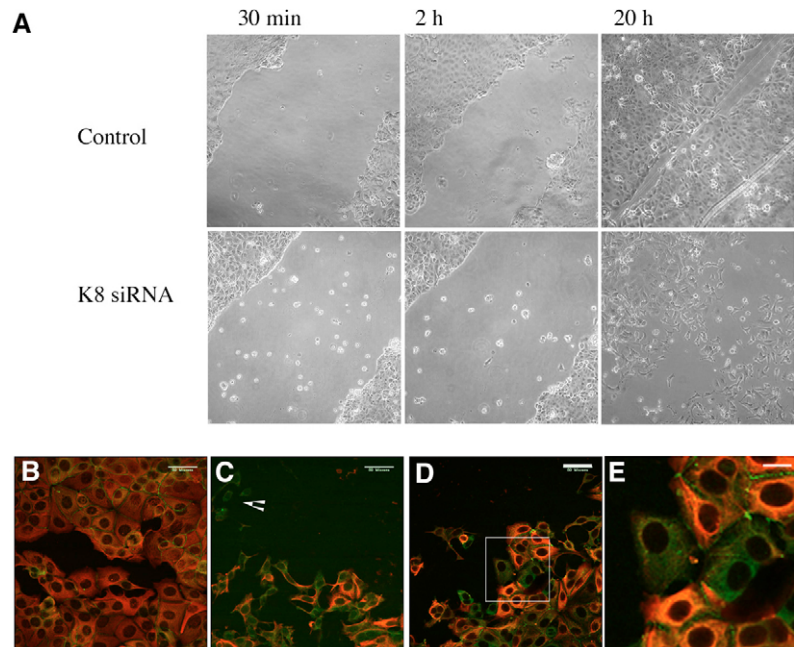
Table 1. The siRNA oligonucleotides used in this study

siRNA oligo	Sequence (5' to 3')	Target region	Knockdown efficiency
Pp11	AUGUAUAAAAUGCUUGGCCtg	C-ter, exon 22	>95%
Pp12	UGCUCGUUUUCCGGUUGGtg	N-ter, exon 15	>95%
Pp13	GAGGGUAUGUAUAAAAUGCtt	C-ter, exon 22	>95%
K8-1	CAUGUUGCUUCGAGCCGUCtt	N-ter head domain	50-80%
K8-2	AAUAUCCUCGUACUGUGCCtt	Rod, exon 6	<5%

close the wound in MCF-7 epithelial sheets (Fig. 8A). It appeared that these individually migrating cells did not maintain the directionality of movement, which was evidenced by observations of K8 negative cells that were simultaneously extending lamellipodia towards both wound edges in the open wound area (data not shown). The control siRNA transfected wounds remained epithelial throughout the closure and retained desmosomes as evidenced by cell border staining for desmoplakin (Fig. 8B). K8 siRNA downregulation resulted in re-distribution of both desmoplakin (Fig. 8C) and periplakin (Fig. 8D) staining to a diffuse cytoplasmic pattern. This is further illustrated in a magnified section of periplakin staining (Fig. 8E), where non-transfected cells retain the keratin IF network and junctional periplakin staining between them, whereas cells without keratin immunoreactivity have almost solely cytoplasmic distribution of periplakin, losing cell-cell contacts with neighbouring cells (Fig. 8E). Although keratin downregulated cells could adopt a more mesenchymal morphology and migrate alone in the wound space leaving the remainder of the epithelial front behind (arrowhead in Fig. 8C), they remained vimentin negative and were not invasive in collagen gel invasion assays (not show). Thus, compared with periplakin knockdown (Fig. 7), keratin knockdown has a more profound effect on epithelial wound healing because of the mistargeting of desmoplakin and periplakin.

To investigate whether keratin intermediate filaments are required for formation or maintenance of desmosomes in other epithelial cell lines, we ablated K8 expression in HeLa and Panc-1 cells (Fig. 9). Control siRNA transfected HeLa cells formed punctate desmoplakin staining at cell borders (Fig. 9A) whereas siRNA knockdown of Keratin 8 abolished cell-border localisation of desmoplakin to a large extent (Fig. 9A). In the control transfected HeLa monolayers that were fixed and scored 30 minutes after scratch wounding, 95% of the cell borders ($n=73$) retained desmosomal localisation of desmoplakin whereas in Keratin-8 siRNA transfected monolayers the corresponding percentage was only 6% ($n=107$). Interestingly, in a transfection where a small island of HeLa cells had remained untransfected and retained prominent K8 expression, punctate desmosomal staining was retained only between keratin-positive cells but not between two knockdown cells or a knockdown cell and a keratin positive cell (Fig. 9A, bottom panels). Western blotting confirmed the successful downregulation of K8 expression (Fig. 9B). It should be noted that both HeLa and Panc-1 cells, unlike MCF-7 cells are vimentin positive (Fig. 9B and data not shown). Loss of desmoplakin localisation at cell borders was also observed in Panc-1 cells transfected with K8 siRNA (Fig. 9C,D). Punctate desmosomal staining was seen only between K8 positive cells, whereas virtually no desmoplakin staining was found at cell borders of K8 knockdown cells (Fig. 9D).

Fig. 8. Wound closure in Keratin 8 siRNA downregulated MCF-7 epithelial sheets. (A) Phase contrast micrographs of the closure of control or K8 siRNA wounds at indicated time points. Cell layers were wounded 48 hours after transfection. Note the loss of epithelial phenotype in K8 siRNA transfected cells at the 20 hours time point. (B) Keratin (red) and desmoplakin (green) immunofluorescence of a control siRNA transfected wound. (C) Keratin (red) and desmoplakin (green) immunofluorescence of a K8 siRNA transfected wound. Arrowhead indicates a group of cells with no keratin immunofluorescence that have migrated away from the cell front to wound space. (D) Keratin (red) and Periplakin (green) immunofluorescence of K8 siRNA transfected wound. (E) Magnification of the area boxed in D. Note, how cells with low keratin expression have mostly cytoplasmic localisation of periplakin. Scale bar in B-D is 50 μm and in E 17 μm .



Furthermore, scratch wound edges of both cell lines were irregular after K8 siRNA transfection and frequently contained cells that were migrating individually (Fig. 9E). Notably, K8 knockdown increased the wound closure rate of both HeLa and Panc-1 cell lines (Fig. 9F), which supports the observation of individual keratin-negative cells escaping the wound edge in MCF-7 cell line.

Discussion

Keratin cytoskeleton is re-arranged at the edge of epithelial wounds

To enable uniform movement that minimises any additional stress by localised cell stretching, migrating epithelial sheets need to maintain cell-cell contacts and synchronize cytoskeletal reorganisation at the moving front. In this report, we present evidence that keratin K8 containing IF network is essential for the integrity of migrating MCF-7 mammary epithelial cells and that periplakin, a cytoskeletal linker protein participates in the organisation of the keratin network.

Firstly, we found that the keratin network is re-organised at the wound edge into thick bundles parallel to the free edge of the epithelial sheet. Keratin cables have been previously reported at the edges of embryonic wounds, which also assemble an actin purse-string (Brock et al., 1996). Actin filaments can serve as a template for keratin organisation in cell-free *Xenopus* egg extracts (Weber and Bement, 2002) and inward-directed movement of keratin particles can depend on intact microfilament network (Werner et al., 2004). Thus, it is possible that after the rapid initial wound response to assemble an actin-purse string, the actin structure is subsequently used to guide the re-organisation of keratins that enforce the free edge of the epithelial sheet.

Live-cell imaging experiments have indicated that IF networks are highly dynamic structures with constant turnover in cells (Windhoffer and Leube, 1999; Liovic et al., 2003; Yoon et al., 2001; Werner et al., 2004). Our results suggest that the keratin network is more dynamic at wound edge cells than in intact monolayer. Wound edge cells appeared to be more vulnerable to okadaic acid treatment (seen in e.g. Fig. 4G) and the ectopic expression of the periplakin C-terminus mostly affected keratin organisation at wound edges (Fig. 5).

Periplakin participates in re-organisation of keratin intermediate filament network

Our results indicate that periplakin participates in the re-organisation of keratins at wound edge. Firstly, siRNA downregulation of periplakin inhibits the re-arrangement of keratin filaments to bundles parallel to the wound edge and impairs wound closure (Fig. 7). Secondly, stable expression of the IF-binding domain of periplakin has an effect on keratin organisation at the wound edge and, consequently, delays wound closure (Fig. 5). The interaction between the cytoplasmic pool of periplakin and IFs appears to be regulated. As shown in Fig. 3, a substantial proportion of total periplakin in MCF-7 cells is found in the soluble cytoplasmic pool where it does not, however, co-localise with IFs. Okadaic acid-treatment that causes disassembly of IFs results in co-aggregation of periplakin with keratins. This interaction is mediated by the periplakin C-terminus. It has been previously shown that plectin is selectively associated with Vanadate-induced keratin granules but not to OA-induced aggregates (Strnad et al., 2002). Thus the phosphorylation status of IFs may selectively regulate their association with different plakin family members. This hypothesis is supported by the increased keratin phosphorylation at the Ser 431 residue in the stable cell line expressing periplakin C-terminus (Fig. 5).

Recently, the periplakin C-terminus has been shown to interact with other proteins in addition to IFs. These binding partners include periphilin, a protein that can also be targeted to nucleus (Kazerounian and Aho, 2003), and Fc γ RI (CD64), that appears to be regulated by binding to periplakin (Beekman et al., 2004). It is not yet known whether these interactions and IF binding are mutually exclusive, but it is conceivable that different periplakin fractions in the cell are engaged with unique functions and interactions. Furthermore, a novel desmosomal protein, kazrin, has recently been identified as an interacting partner for periplakin N-terminus and may mediate localization of periplakin (Groot et al., 2004).

Another plakin family member, epiplakin, has recently been implicated in organisation of IF networks. Knockdown of

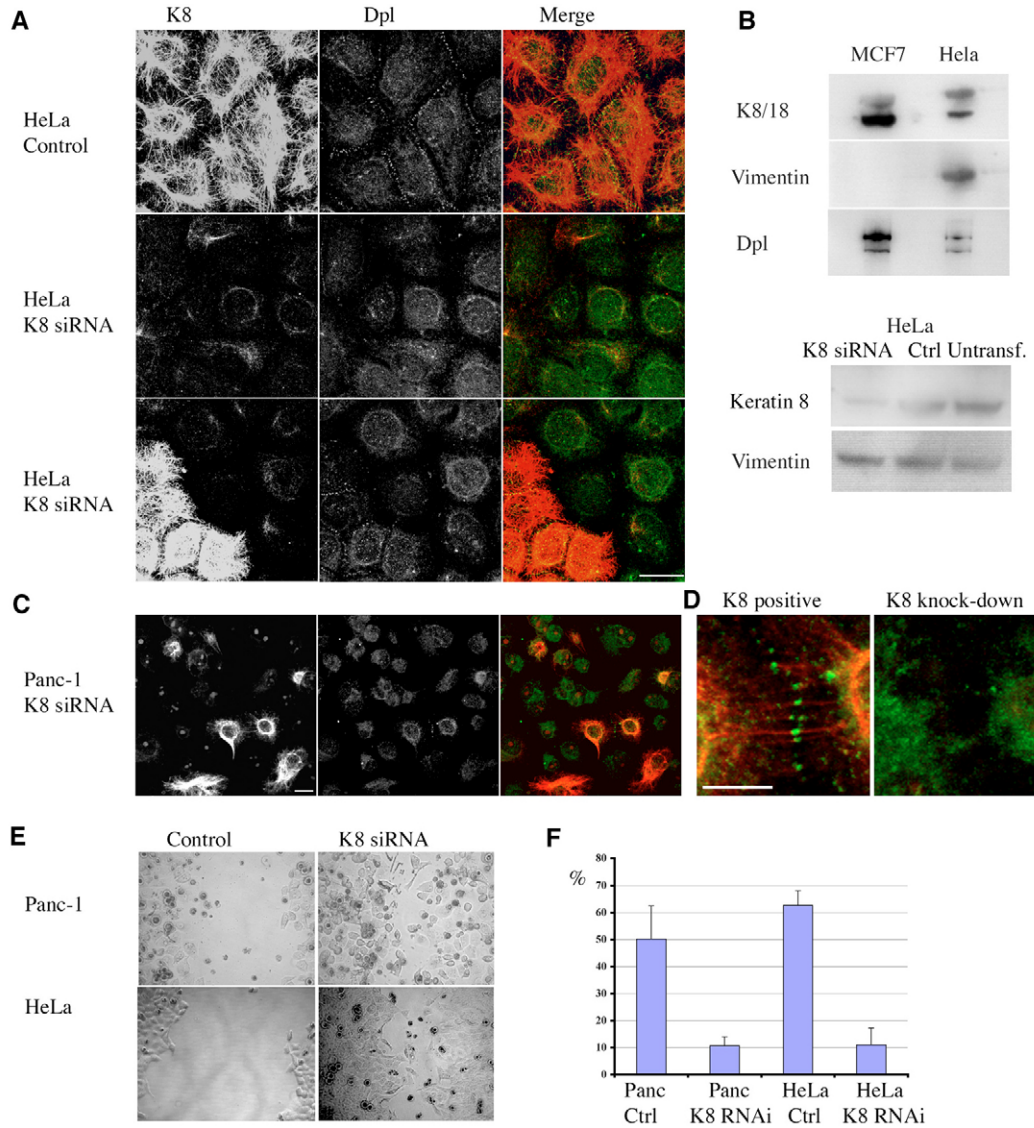


Fig. 9. K8 knockdown and wound closure in HeLa and Panc-1 cell lines. (A) Control and K8 siRNA transfected HeLa monolayers. Red channel (left), K8 immunofluorescence, green (middle) desmoplakin immunofluorescence and merged image (right) are shown. (B) Western blotting of keratin and vimentin expression in the transfected cells. HeLa cells are vimentin positive but express both keratin 8 and desmoplakin. siRNA transfection effectively knocks down K8 expression in 72 hours. (C) Panc-1 monolayer transfected with K8 siRNA and stained for K8 (red) and desmoplakin. (D) Higher magnification example of desmoplakin (green) staining at Panc 1 cell borders showing punctate desmosomal staining between K8-positive (red, left panel) but not between K8 knockdown cells (right panel). (E) Phase-contrast micrographs of scratch wound closure (20 hours time-point) in Panc-1 and HeLa monolayers transfected with control or K8 siRNA oligonucleotides. Note that the wounds in Panc-1 and HeLa monolayers were wider than in experiments with MCF-7 cells. (F) Quantification of the wound closure. Open wound at 20 hours time point was measured from photomicrographs (six measurements each from two transfections for both cell lines). Scale bar: 20 μ m in A and C; 5 μ m in D.

epiplakin in simple epithelial cells results in disruption of keratin and vimentin networks (Jang et al., 2005). Thus, siRNA experiments indicate that epiplakin is required for maintenance of simple epithelial keratin network, whereas peri-plakin is involved in keratin bundling at epithelial wound edge.

Downregulation of K8 expression by siRNA transfection results in a loss of epithelial integrity

Our results indicate that knockdown of K8 network in migrating epithelia results in a loss of epithelial integrity and affects wound closure. The role of keratins in collective

epithelial migration has been previously studied mainly in the context of epidermal keratinocytes and skin wound healing. Gene targeting of both K6a and K6b keratins increases keratinocyte outgrowth in skin explant assays but impairs wound healing in vivo owing to increased fragility of mutant keratinocytes (Wong and Coulombe, 2003). In our experiments, the MCF-7 cells with lowest level of keratin expression appeared to escape from the migrating cell front and K8-ablated HeLa and Panc-1 cells migrated faster than control transfected cells (Figs 8 and 9). Likewise, epidermolysis bullosa simplex cell lines carrying K14 mutations display fast

migration in vitro (Morley et al., 2003). Taken together, it appears that keratin network can regulate the collective motility of epithelial sheets to maintain epithelial integrity and to withstand tensile stress during migration. This is supported by experiments that directly measured traction forces in migrating epithelium (du Roure et al., 2005). The maximum intensity of the force was found at the edge of migrating MDCK epithelia (du Roure et al., 2005). It is likely that the assembly of the keratin cable is a strengthening response that protects the epithelia against these forces.

There is a difference between our results and the outcome of embryonic wound healing in K8 null mice. In the C57/B1 genetic background, K8 deficiency leads to embryonic lethality (Baribault et al., 1993), whereas the same mutation in FVB/N background results in viable animals (Baribault et al., 1994). When embryonic wound healing was investigated in K8^{-/-} mice in FVB/N background, no difference in the wound closure was observed between gene targeted and wild type embryos (Brock et al., 1996). On the contrary, *Xenopus* embryos depleted from maternal keratins fail to undergo normal morphogenetic tissue movements and have a defect in epithelial wound healing (Torpey et al., 1992; Klymkowsky et al., 1992). It is possible that there are subtle species or cell-type specific differences in the requirement for keratins in epithelial migration. It is also notable, that the study by Brock et al. (Brock et al., 1996) only investigated embryonic wound healing in the genetic background that supports the survival of mK8^{-/-} embryos.

Our results also support the concept that IFs are involved in correct subcellular targeting of desmosomal proteins. RNAi-mediated depletion of K8 resulted in a breakdown of cell-cell adhesions and re-distribution of desmoplakin and periplakin from cell borders to cytosol (Figs 6, 8 and 9). The recruitment of desmoplakin to cell borders occurs in three phases and both microfilaments and IFs are involved in targeting of cytoplasmic particles containing desmoplakin and plakophilin-2 to maturing borders. Specific DP mutants that either increase or abrogate the association of DP with keratins delayed incorporation of DP particles into junctions (Godsel et al., 2005). Furthermore, in A431 epithelial cells, an inducible expression of desmoplakin N-terminal domain severs the connection of IFs to desmosomes and results in dissociation of epithelial sheets subjected to mechanical stress (Huen et al., 2002). Notably, we found that both vimentin negative MCF-7 cells and vimentin positive HeLa and Panc-1 cells fail to target desmoplakin at cell borders. The role of keratins in the maintenance of desmosomes is also supported by findings of a careful histological characterisation of liver lesions in both K8 and K18 null mice (Toivola et al., 2001). Livers of keratin null mice showed large areas that were devoid of both desmoplakin and filamentous actin staining (Toivola et al., 2001). One possible reason for mistargeting of desmoplakin in the absence of keratins could be altered function of plakophilins in the recruitment of desmoplakin. Plakophilins bind and bundle intermediate filaments in vitro (Hofmann et al., 2000) and plakophilin-1 and 2 mutations or deficiency can result in altered targeting of desmoplakin in skin and cardiac muscle, respectively (McGrath et al., 1997; Grossmann et al., 2004).

In summary, we suggest that periplakin is a cytoskeletal linker protein that acts as an organiser of intermediate filament architecture during cell migration. Furthermore, our work

supports the view that intermediate filaments can serve a structural role in simple epithelial cells by contributing to maintenance of the epithelial integrity during collective migration.

Materials and Methods

Cell culture and scratch wound assays

MCF-7, HeLa and Panc-1 cells were maintained in DMEM (Sigma, UK) supplemented with 5% v/v antibiotics (penicillin and streptomycin, Sigma) L-glutamate and 10% foetal calf serum (Sigma). For okadaic acid (OA) treatment, MCF-7 cells were incubated with 500 nM OA (Calbiochem) for 2 hours and for SB203580 treatment with 20 μ M SB203580 (Calbiochem) for 2 hours. Cells were incubated with 1% v/v DMSO as a control. For scratch wound assays, cells were grown to 100% confluence and wounded using a 200 μ l pipette tip.

Transient and stable plasmid transfections

Cells were grown to 40-50% confluence on glass coverslips and transfected with 1 μ g of plasmid vectors using Genejuice[®] (Novagen). The cells were processed for immunofluorescence or protein extraction 48 hours post-transfection. To generate stable cell lines, MCF-7 cells were transfected with pCI-neo mammalian expression vector (Promega). Cells were allowed to recover for 48 hours before selection with neomycin (500 μ g ml⁻¹). Neomycin-resistant colonies were expanded and analysed by immunoblotting, immunofluorescence and immunoprecipitation. Two independent clones were used in subsequent experiments.

Transient siRNA transfections

Double-stranded siRNA oligonucleotides against K8 and periplakin and a negative scrambled control were purchased from Ambion (Table 1). Cells were prepared for transfection as before and 60 nmol of siRNA oligonucleotides were transfected using Oligofectamine (Invitrogen). Cells were processed for immunofluorescence or protein extraction 48-72 hours after transfection. CellTiter 96[®] AQueous One Solution Cell Proliferation Assay (Promega) was modified to assess the cell survival 3 days after siRNA transfection. Cells were plated at 50% confluency in 12 well plates and transfected in triplicates with siRNA. Three 100 μ l aliquots from each transfected well were analysed at 490 nm with a spectrophotometric plate reader (AnthosLucy1).

Live cell imaging

MCF-7 cells were seeded on glass bottom 3 cm² dishes (Iwaki) and transfected with pEGFP-Cter or with empty pEGFP-N vector. Live cell imaging was performed using an Olympus wide field microscope equipped with DeltaVision RT imaging system with deconvolution software (Applied Precision, UK). Images were taken using a 63 \times objective at 5 minutes intervals over a 2 hour period in a 37°C environment. After first imaging the cells for a period of 10 minutes, the cells were treated with OA (500 nM final concentration). Deconvoluted images were saved as Quicktime movies and series of still images using Softworks software (Applied Precision, UK).

Immunofluorescence analysis

The following antibodies were used: LE41 [1:2 dilution of supernatant; mouse mAb to K8 and 18 (Lane et al., 1982)]; AHP320 (1:100, rabbit polyclonal to desmoplakin, Serotec); DP1/2 (1:100, mouse mAb to desmoplakin, ICN); 5B3 (1:100, mouse mAb to K8 phosphoserine residue 431, Stratech); LJ4 (1:100, mouse mAb to K8 phosphoserine residue 73, Stratech); TD2 (1:100, rabbit polyclonal to periplakin) (Määttä et al., 2001); and β Cat (1:500, mouse mAb to β -catenin, BD BioScience). The cells were fixed with ice-cold methanol/acetone (1:1, v/v) for 15 minutes at room temperature or in 4% paraformaldehyde for 10 minutes. The paraformaldehyde fixed cells were permeabilized with 1% NP40 for 10 minutes; blocked with 0.5% fish skin gelatin (Sigma) and incubated with primary antibodies for 1 hour. Primary antibodies were detected using the Alexa[®] 488 green (Invitrogen) conjugated anti-mouse secondary antibody (1:800) and 594 red (Invitrogen) conjugated anti-rabbit Alexa[®] secondary antibody (1:800). Filamentous actin was stained with FITC-labelled phalloidin (Sigma). The coverslips were mounted on slides using Citifluor[®] (Citifluor Labs, UK). Cells were observed with Zeiss LSM 510 Zeiss or BioRad Radiance 2000 laser scanning confocal microscopes. Composite images were assembled using Adobe[®] Photoshop 7.0 (Adobe Systems) and LSM510 image browser software (Carl Zeiss).

Detergent subcellular fractionation of proteins

MCF-7 cells were grown to confluence on 10cm² dishes and extracted using saponin as described (Palka and Green, 1997). Briefly, cells were extracted in saponin buffer (0.01% w/v saponin, 10 mM Tris pH 7.5, 140 mM NaCl, 5 mM EDTA, 2 mM EGTA, 1 mM PMSF and protease inhibitor cocktail tablets (Roche) on ice for 10 minutes and centrifuged at 14,000 g for 30 minutes, 4°C. The saponin-insoluble pellet was further extracted using ice-cold Triton buffer (1%v/v Triton X-100, 10 mM Tris pH 7.5, 140 mM NaCl, 5 mM EDTA, 2 mM EGTA, 1 mM PMSF and protease inhibitor cocktail). After vortexing the pellet for 30 seconds, the Triton

fraction was centrifuged for 30 minutes at 14,000 *g* at 4°C to separate the Triton-soluble and insoluble fractions. All the fractions were adjusted to the same volume before analysis by immunoblotting.

Immunoblotting

The following antibodies were used in addition to those described above; Ab-2 (mouse monoclonal to K18, oncogene) and AE3 (mouse monoclonal to K8, abcam). To analyse plakin proteins cell extracts were electrophoresed in 4-12% Bis-Tris pre-cast gels (Invitrogen) and transferred onto nitrocellulose membranes (VWR). The protein bands were visualised using the enhanced chemiluminescence reaction (ECL, GE Healthcare) and Fuji image LAS-1000 intelligent dark box.

Membrane extraction, actin depletion and scanning electron microscopy

To visualise the intermediate filament network with scanning electron microscopy, the method of Svitkina et al. (Svitkina et al., 1996) was used with a few modifications. Briefly, MCF-7 cells were grown on silicon chips (Agar Scientific, UK). After scratch wounding, the cells were extracted in 1% Triton X-100, 4% PEG (40,000 *M_r*), 50 mM imidazole, pH 6.8, 50 mM KCl, 0.5 mM MgCl₂, 0.1 mM EDTA, 0.1 mM EGTA for 5 minutes at room temperature and washed in cytoskeleton buffer M (50 mM imidazole, pH 6.8, 50 mM KCl, 0.5 mM MgCl₂, 0.1 mM EDTA, 0.1 mM EGTA). To remove filamentous actin, the extracted cells were rinsed in buffer G (50 mM MES-KOH, pH 6.3, 0.1 mM CaCl₂, 2 mM MgCl₂, and 0.5 mM DTT), incubated with 0.1 mg ml⁻¹ of purified human gelsolin in buffer G (Cytoskeleton) for 1 hour at room temperature and finally rinsed in buffer M. The cells were fixed in 2% glutaraldehyde in 0.1 M sodium cacodylate, pH 7.3 overnight at 4°C, warmed to room temperature, incubated in 0.1% aqueous tannic acid for 20 minutes and processed for electron microscopy. Critical point drying was performed using a Baltec critical point dryer (Baltec). Dried samples were rotary shadowed with Chromium using a Cressington Chromium sputter coater (Cressington, UK) and examined in a Hitachi S-5200 Ultra-high resolution scanning electron microscope (Nissei Sangyo America, Ltd).

This work was supported by a BBSRC grant. V.B. is supported by a British Skin Foundation studentship and L.M. is supported by a Cancer Research UK William Ross Studentship. We are grateful to Fiona Watt (CRUK, London Institute) for providing TD2 antibody and HA-tagged periplakin constructs, to Birgit Lane for keratin 8 monoclonal antibody and to Nkemcho Ojeh, Adam Benham and Roy Quinlan for valuable comments on the manuscript.

References

- Abrahamsberg, C., Fuchs, P., Osmanagic-Myers, S., Fischer, I., Propst, F., Elbe-Burger, A. and Wiche, G. (2005). Targeted ablation of plectin isoform 1 uncovers role of cytolinker proteins in leukocyte recruitment. *Proc. Natl. Acad. Sci. USA* **102**, 18449-18454.
- Aho, S., McLean, W. H., Li, K. and Uitto, J. (1998). cDNA cloning, mRNA expression, and chromosomal mapping of human and mouse periplakin genes. *Genomics* **48**, 242-247.
- Andra, K., Nikolic, B., Stocher, M., Drenckhahn, D. and Wiche, G. (1998). Not just scaffolding: plectin regulates actin dynamics in cultured cells. *Genes Dev.* **12**, 3442-3451.
- Baribault, H., Price, J., Miyai, K. and Oshima, R. G. (1993). Mid-gestational lethality in mice lacking keratin 8. *Genes Dev.* **7**, 1191-1202.
- Baribault, H., Penner, J., Iozzo, R. V. and Wilson-Heiner, M. (1994). Colorectal hyperplasia and inflammation in keratin 8-deficient mice. *Genes Dev.* **8**, 2964-2973.
- Beekman, J. M., Bakema, J. E., van de Winkel, J. G. and Leusen, J. H. (2004). Direct interaction between FcγRI (CD64) and periplakin controls receptor endocytosis and ligand binding capacity. *Proc. Natl. Acad. Sci. USA* **101**, 10392-10397.
- Beil, M., Micoulet, E., von Wichert, G., Paschke, S., Walther, P., Omary, M. B., Van Veldhoven, P. P., Gern, U., Wolff-Hiebe, E., Eggermann, J. et al. (2003). Sphingosylphosphorylcholine regulates keratin network architecture and visco-elastic properties of human cancer cells. *Nat. Cell Biol.* **5**, 803-811.
- Bement, W. M., Forscher, P. and Mooseker, M. S. (1993). A novel cytoskeletal structure involved in purse string wound closure and cell polarity maintenance. *J. Cell Biol.* **121**, 565-578.
- Brock, J., McCluskey, J., Baribault, H. and Martin, P. (1996). Perfect wound healing in the keratin 8 deficient mouse embryo. *Cell Motil. Cytoskeleton.* **35**, 358-366.
- Chang, L. and Goldman, R. D. (2004). Intermediate filaments mediate cytoskeletal crosstalk. *Nat. Rev. Mol. Cell Biol.* **5**, 601-613.
- Chu, Y. W., Runyan, R. B., Oshima, R. G. and Hendrix, M. J. (1993). Expression of complete keratin filaments in mouse L cells augments cell migration and invasion. *Proc. Natl. Acad. Sci. USA* **90**, 4261-4265.
- Chu, Y. W., Seftor, E. A., Romer, L. H. and Hendrix, M. J. (1996). Experimental coexpression of vimentin and keratin intermediate filaments in human melanoma cells augments motility. *Am. J. Pathol.* **148**, 63-69.
- Danjo, Y. and Gipson, I. K. (1998). Actin 'purse string' filaments are anchored by E-cadherin-mediated adherens junctions at the leading edge of the epithelial wound, providing coordinated cell movement. *J. Cell Sci.* **111**, 3323-3332.
- DiColandrea, T., Karashima, T., Määttä, A. and Watt, F. M. (2000). Subcellular distribution of envoplakin and periplakin: insights into their role as precursors of the epidermal cornified envelope. *J. Cell Biol.* **151**, 573-586.
- du Roure, O., Saez, A., Austin, R. H., Chavrier, P., Silberzan, P. and Ladoux, B. (2005). Force mapping in epithelial cell migration. *Proc. Natl. Acad. Sci. USA* **102**, 2390-2395.
- Fenteany, G., Janmey, P. A. and Stossel, T. P. (2000). Signaling pathways and cell mechanics involved in wound closure by epithelial cell sheets. *Curr. Biol.* **10**, 831-838.
- Friedl, P., Hegerfeldt, Y. and Tusch, M. (2004). Collective cell migration in morphogenesis and cancer. *Int. J. Dev. Biol.* **28**, 441-449.
- Gallicano, G. I., Kouklis, P., Bauer, C., Yin, M., Vasioukhin, V., Degenstein, L. and Fuchs, E. (1998). Desmoplakin is required early in development for assembly of desmosomes and cytoskeletal linkage. *J. Cell Biol.* **143**, 2009-2022.
- Godsel, L. M., Hsieh, S. N., Amargo, E. V., Bass, A. E., Pascoe-McGillicuddy, L. T., Huen, A. C., Thorne, M. E., Gaudry, C. A., Park, J. K., Myung, K. et al. (2005). Desmoplakin assembly dynamics in four dimensions: multiple phases differentially regulated by intermediate filaments and actin. *J. Cell Biol.* **171**, 1045-1059.
- Groot, K. R., Sevilla, L. M., Nishi, K., DiColandrea, T. and Watt, F. M. (2004). Kazrin, a novel periplakin-interacting protein associated with desmosomes and the keratinocyte plasma membrane. *J. Cell Biol.* **166**, 653-659.
- Grossmann, K. S., Grund, C., Huelsken, J., Behrend, M., Erdmann, B., Franke, W. W. and Birchmeier, W. (2004). Requirement of plakophilin 2 for heart morphogenesis and cardiac junction formation. *J. Cell Biol.* **167**, 149-160.
- Guo, L., Degenstein, L., Dowling, J., Yu, Q. C., Wollmann, R., Perman, B. and Fuchs, E. (1995). Gene targeting of BPAG1: abnormalities in mechanical strength and cell migration in stratified epithelia and neurologic degeneration. *Cell* **81**, 233-243.
- Hofman, I., Mertens, C., Brettel, M., Nimmrich, V., Schnolzer, M. and Herrmann, H. (2000). Interaction of plakophilins with desmoplakin and intermediate filament proteins: an in vitro analysis. *J. Cell Sci.* **113**, 2471-2483.
- Huen, A. C., Park, J. K., Godsel, L. M., Chen, X., Bannon, L. J., Amargo, E. V., Hudson, T. Y., Mongiu, A. K., Leigh, I. M., Kessel, D. P. et al. (2002). Intermediate filament-membrane attachments function synergistically with actin-dependent contacts to regulate intercellular adhesive strength. *J. Cell Biol.* **159**, 1005-1017.
- Jang, S.-I., Kalinin, A., Takahashi, K., Marekov, L. N. and Steinert, P. M. (2005). Characterisation of human epiplakin: RNAi-mediated epiplakin depletion leads to the disruption of keratin and vimentin IF networks. *J. Cell Sci.* **118**, 781-793.
- Karashima, T. and Watt, F. M. (2002). Interaction of periplakin and envoplakin with intermediate filaments. *J. Cell Sci.* **115**, 5027-5037.
- Kazerounian, S. and Aho, S. (2003). Characterization of periphilin, a widespread, highly insoluble nuclear protein and potential constituent of the keratinocyte cornified envelope. *J. Biol. Chem.* **278**, 36707-36717.
- Kazerounian, S., Uitto, J. and Aho, S. (2002). Unique role for the periplakin tail in intermediate filament association: specific binding to keratin 8 and vimentin. *Exp. Dermatol.* **11**, 428-438.
- Klymkowsky, M. W., Shook, D. R. and Maynell, L. A. (1992). Evidence that the deep keratin filament systems of the *Xenopus* embryo act to ensure normal gastrulation. *Proc. Natl. Acad. Sci. USA* **89**, 8736-8740.
- Lane, E. B. (1982). Monoclonal antibodies provide specific intramolecular markers for the study of epithelial tonofilament organization. *J. Cell Biol.* **92**, 665-673.
- Leung, C. L., Green, K. J. and Liem, R. K. (2002). Plakins: a family of versatile cytolinker proteins. *Trends Cell Biol.* **12**, 37-45.
- Liao, J., Ku, N. O. and Omary, M. B. (1997). Stress, apoptosis, and mitosis induce phosphorylation of human keratin 8 at Ser-73 in tissues and cultured cells. *J. Biol. Chem.* **272**, 17565-17573.
- Liovic, M., Morgensen, M. M., Prescott, A. R. and Lane, E. B. (2003). Observation of keratin particles showing fast bidirectional movement colocalized with microtubules. *J. Cell Sci.* **116**, 1417-1427.
- Määttä, A., DiColandrea, T., Groot, K. and Watt, F. M. (2001). Gene targeting of envoplakin, a cytoskeletal linker protein and precursor of the epidermal cornified envelope. *Mol. Cell Biol.* **21**, 7047-7053.
- Martin, P. and Lewis, J. (1992). Actin cables and epidermal movement in embryonic wound healing. *Nature* **360**, 179-183.
- Martin, P. and Parkhurst, S. M. (2004). Parallels between tissue repair and embryo morphogenesis. *Development* **131**, 3021-3034.
- McGrath, J. A., McMillan, J. R., Shemanko, C. S., Runswick, S. K., Leigh, I. M., Lane, E. B., Garrod, D. R. and Eady, R. A. J. (1997). Mutations in the plakophilin 1 gene result in ectodermal dysplasia/skin fragility syndrome. *Nature Genetics* **17**, 240-244.
- Morley, S. M., D'Alessandro, M., Sexton, C., Rugg, E. L., Navsaria, H., Shemanko, C. S., Huber, M., Hohl, D., Heagerty, A. L., Leigh, I. M. and Lane, E. B. (2003). Generation and characterization of epidermolysis bullosa simplex cell lines: scratch assays show faster migration with disruptive keratin mutations. *Br. J. Dermatol.* **149**, 46-58.
- Owens, D. W. and Lane, E. B. (2003). The quest for the function of simple epithelial keratins. *BioEssays* **25**, 748-758.
- Palka, H. L. and Green, K. J. (1997). Roles of plakoglobin end domains in desmosome assembly. *J. Cell Sci.* **110**, 2359-2371.
- Ruhrberg, C., Hajibagheri, M. A., Parry, D. A. and Watt, F. M. (1997). Periplakin, a novel component of cornified envelopes and desmosomes that belongs to the plakin family and forms complexes with envoplakin. *J. Cell Biol.* **139**, 1835-1849.
- Salas, P. J., Rodriguez, M. L., Viciano, A. L., Vega-Salas, D. E. and Hauri, H. P.

- (1997). The apical submembrane cytoskeleton participates in the organization of the apical pole in epithelial cells. *J. Cell Biol.* **137**, 359-375.
- Strnad, P., Windoffer, R. and Leube, R. E.** (2001). In vivo detection of cytokeratin filament network breakdown in cells treated with the phosphatase inhibitor okadaic acid. *Cell Tissue Res.* **306**, 277-293.
- Strnad, P., Windoffer, R. and Leube, R. E.** (2002). Induction of rapid and reversible cytokeratin filament network remodeling by inhibition of tyrosine phosphatases. *J. Cell Sci.* **115**, 4133-4148.
- Svitkina, T. M., Verkhovsky, A. B. and Borisy, G. G.** (1996). Plectin sidearms mediate interaction of intermediate filaments with microtubules and other components of the cytoskeleton. *J. Cell Biol.* **135**, 991-1007.
- Toivola, D. M., Nieminen, M. I., Hesse, M., He, T., Baribault, H., Magin, T. M. and Eriksson, J. E.** (2001). Disturbances in hepatic cell-cycle regulation in mice with assembly-deficient keratins 8/18. *Hepatology* **34**, 1174-1183.
- Toivola, D. M., Krishnan, S., Binder, H. J., Singh, S. K. and Omary, M. B.** (2004). Keratins modulate colonocyte electrolyte transport via protein mistargeting. *J. Cell Biol.* **164**, 911-921.
- Toivola, D. M., Tao, G. Z., Habtezion, A., Liao, J. and Omary, M. B.** (2005). Cellular integrity plus: organelle-related and protein-targeting functions of intermediate filaments. *Trends Cell Biol.* **15**, 608-617.
- Torpey, N., Wylie, C. C. and Heasman, J.** (1992). Function of maternal cytokeratin in *Xenopus* development. *Nature* **357**, 413-415.
- Vasioukhin, V., Bowers, E., Bauer, C., Degenstein, L. and Fuchs, E.** (2001). Desmoplakin is essential in epidermal sheet formation. *Nat. Cell Biol.* **312**, 1076-1085.
- Weber, K. L. and Bement, W. M.** (2002). F-actin serves as a template for cytokeratin organization in cell free extracts. *J. Cell Sci.* **115**, 1373-1382.
- Werner, N. S., Windoffer, R., Strnad, P., Grund, C., Leube, R. E. and Magin, T. M.** (2004). Epidermolysis bullosa simplex-type mutations alter the dynamics of the keratin cytoskeleton and reveal a contribution of actin to the transport of keratin subunits. *Mol Biol. Cell.* **15**, 990-1002.
- Windoffer, R. and Leube, R. E.** (1999). Detection of cytokeratin dynamics by time-lapse fluorescence microscopy in living cells. *J. Cell Sci.* **112**, 4521-4534.
- Wong, P. and Coulombe, P. A.** (2003). Loss of keratin 6 (K6) proteins reveals a function for intermediate filaments during wound repair. *J. Cell Biol.* **163**, 327-337.
- Yatsunami, J., Komori, A., Ohta, T., Suganuma, M., Yuspa, S. H. and Fujiki, H.** (1993). Hyperphosphorylation of cytokeratins by okadaic acid class tumor promoters in primary human keratinocytes. *Cancer Res.* **53**, 992-926.
- Yoon, K. H., Yoon, M., Moir, R. D., Khuon, S., Flitney, F. W. and Goldman, R. D.** (2001). Insights into the dynamic properties of keratin intermediate filaments in living epithelial cells. *J. Cell Biol.* **153**, 503-516.
- Zhou, X., Stuart, A., Dettin, L. E., Rodriguez, G., Hoel, B. and Gallicano, G. I.** (2004). Desmoplakin is required for microvascular tube formation in culture. *J. Cell Sci.* **117**, 3129-3140.